

# Effect of the organic functionalization of flexible MOFs on the adsorption of CO<sub>2</sub>

Thomas Devic,<sup>\*a</sup> Fabrice Salles,<sup>b</sup> Sandrine Bourrelly,<sup>c</sup> Béatrice Moulin,<sup>d</sup> Guillaume Maurin,<sup>b</sup> Patricia Horcajada,<sup>a</sup> Christian Serre,<sup>a</sup> Alexandre Vimont,<sup>d</sup> Jean-Claude Lavalley,<sup>d</sup> Hervé Leclerc,<sup>d</sup> Guillaume Clet,<sup>d</sup> Marco Daturi,<sup>d</sup> Phillip Llewellyn,<sup>c</sup> Yaroslav Filinchuk<sup>e</sup> and Gérard Férey<sup>a</sup>

<sup>a</sup> Institut Lavoisier, UMR CNRS 8180, Université de Versailles Saint-Quentin-en-Yvelines, 45 avenue des Etats-Unis, 78035 Versailles cedex, France; E-mail: devic@chimie.uvsq.fr.

<sup>b</sup> Institut Charles Gerhardt Montpellier, UMR CNRS 5253, UM2, ENSCM, Place E. Bataillon, 34095 Montpellier cedex 05 France.

<sup>c</sup> Laboratoire Chimie Provence, UMR 6264, Universités Aix-Marseille I, II & III - CNRS, Centre de Saint Jérôme, 13397 Marseille Cedex 2, France.

<sup>d</sup> Laboratoire Catalyse et Spectrochimie, ENSICAEN, Université de Caen, CNRS, 6 Bd Maréchal Juin, 14050 Caen, France.

<sup>e</sup> Swiss Norwegian Beam Lines at ESRF, 38043 Grenoble, France.

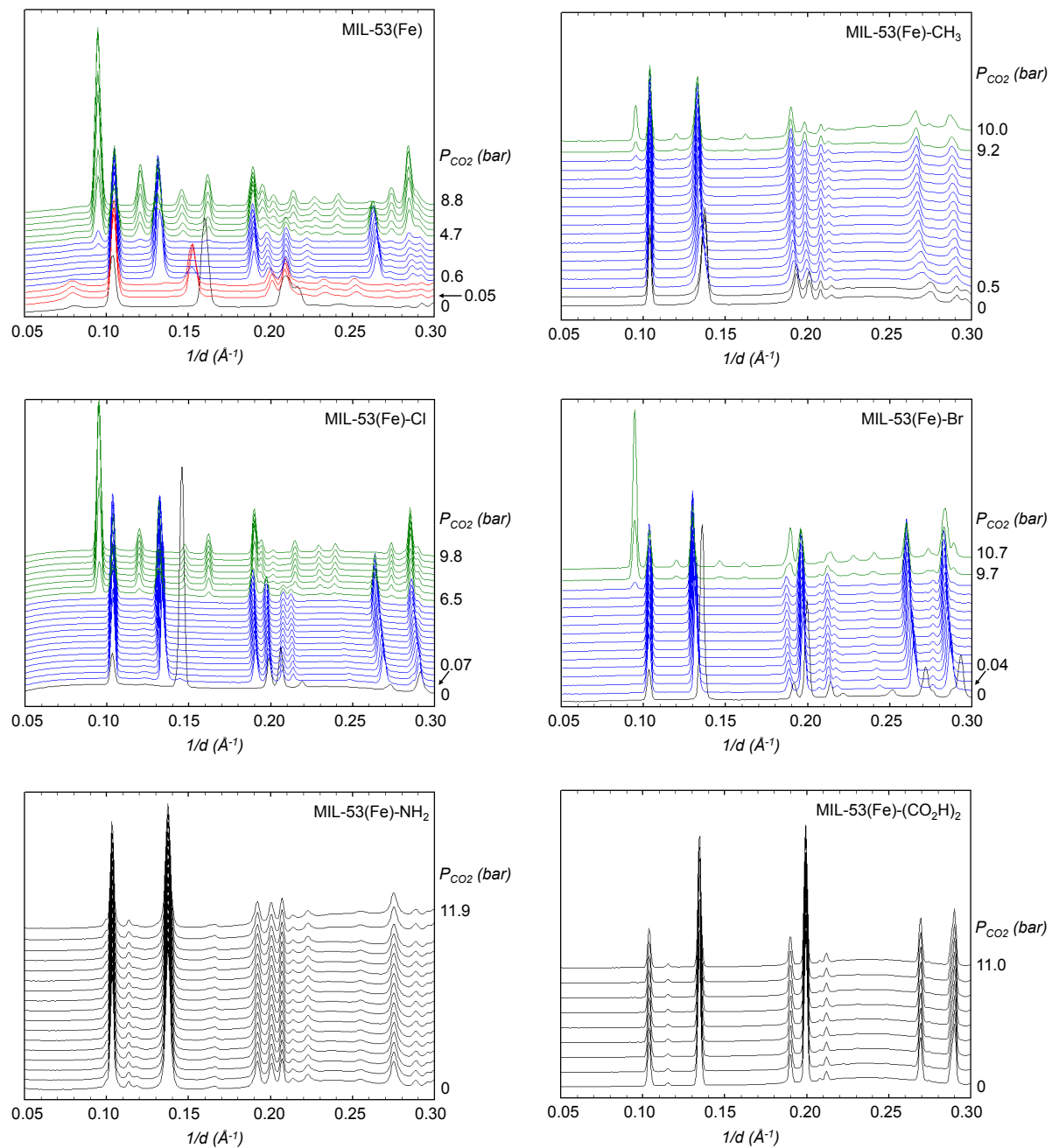


**Figure S1** Adsorption of CO<sub>2</sub> on MIL-53(Fe)-X (X = -, Cl, Br, CH<sub>3</sub>, NH<sub>2</sub>, (CO<sub>2</sub>H)<sub>2</sub>) at 230 K followed by XRPD. The colour corresponds to the major phase observed at the given pressure: black: anhydrous CP form; red: triclinic INT form; blue: NP form, green: LP form.

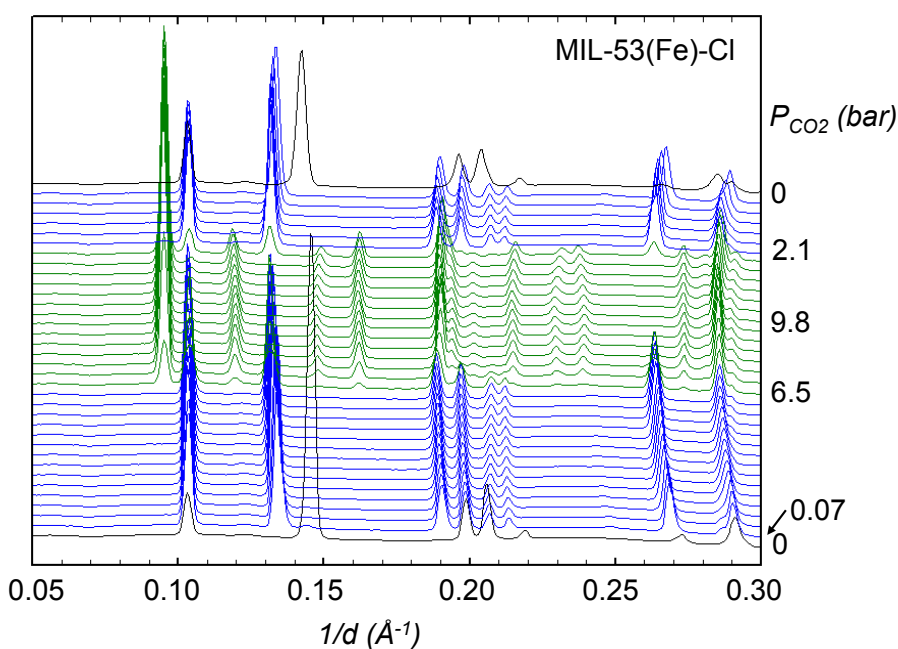


**Figure S2** Adsorption and desorption of  $\text{CO}_2$  on MIL-53(Fe)-Cl at 230 K followed by XRPD.

The colour corresponds to the major phase observed at the given pressure: black: anhydrous CP form; blue: NP form.

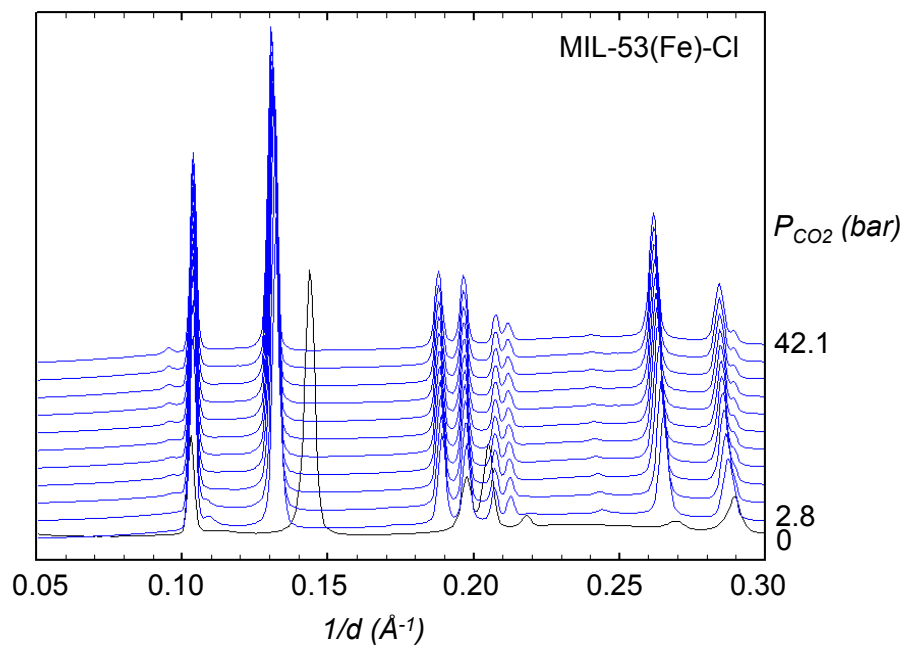


**Figure S3** Adsorption of  $\text{CO}_2$  on MIL-53(Fe)-Cl at 303 K followed by XRPD. The colour corresponds to the major phase observed at the given pressure: black: anhydrous CP form; blue: NP form.

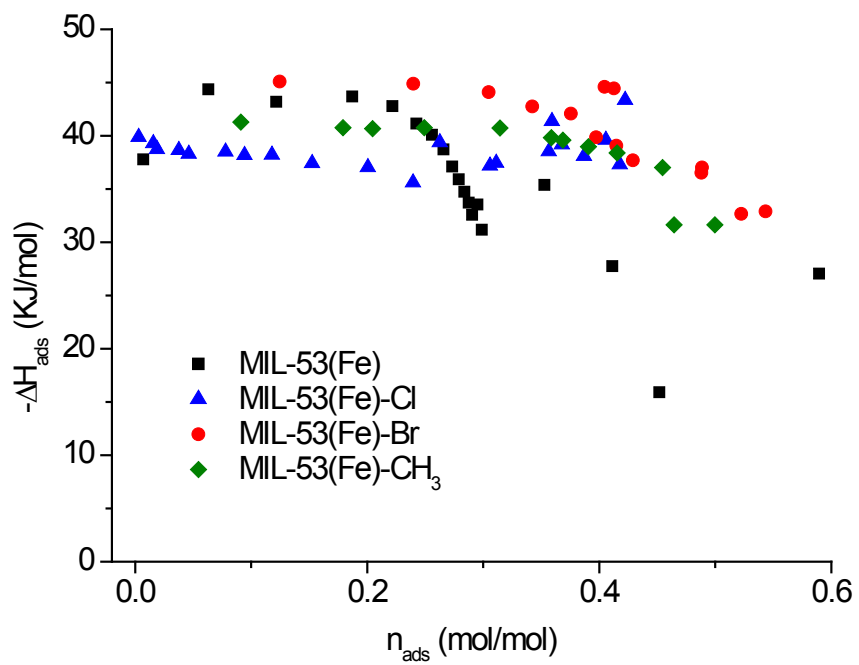


**Figure S4** Differential adsorption enthalpies at 303 K obtained from microcalorimetry measurements for the adsorption of CO<sub>2</sub> on MIL-53(Fe)-X (X = -, Cl, Br, CH<sub>3</sub>).

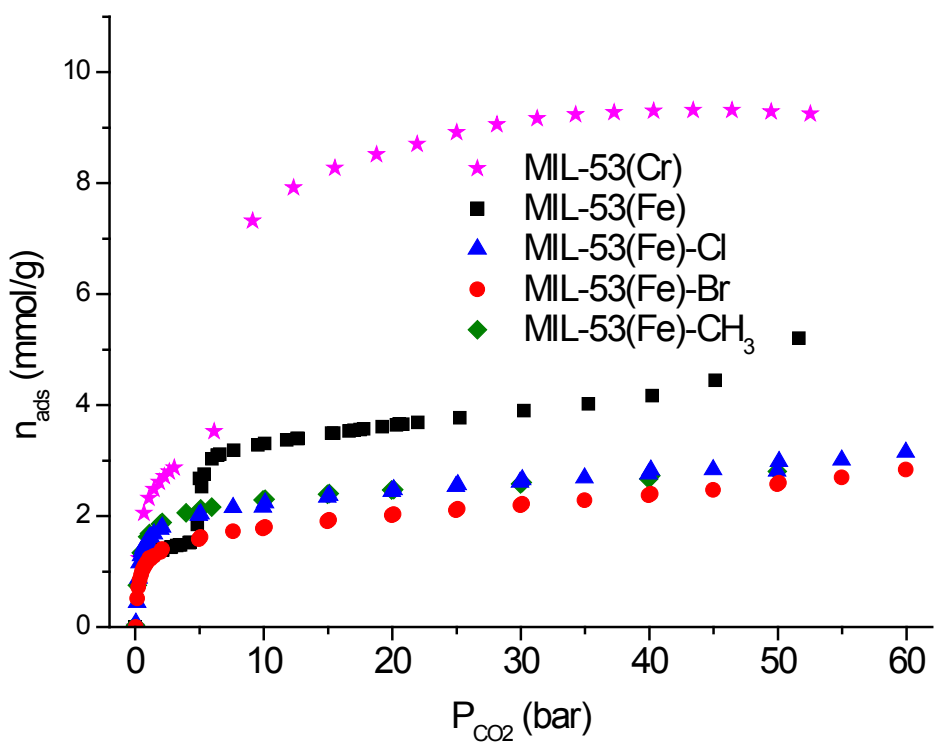


**Figure S5** Adsorption isotherms of CO<sub>2</sub> on MIL-53(Fe)-X (X = -, Cl, Br, CH<sub>3</sub>) at 303 K, reported in mmol/g.

### Estimation of the pore volume of the MIL-53(Fe)-X (X = Cl, Br, CH<sub>3</sub>) from experiments.

The micropore volumes were estimated from the amount of CO<sub>2</sub> adsorbed at 303 K. With the assumption that the volumetric mass of the adsorbed CO<sub>2</sub> is identical to the one of liquid CO<sub>2</sub> at 303 K and 72 bars (591.6 Kg m<sup>-3</sup>), the amount of adsorbed gas was transformed to a volume of adsorbed liquid, which can be assimilated to a micropore volume, following the equation:

$$V_{\text{ads, liq}} = n_{\text{ads}} (\text{mol g}^{-1}) * M_{\text{CO}_2} (\text{g mol}^{-1}) / \rho_{\text{CO}_2} (\text{g cm}^{-3}) = V_{\text{pore}} (\text{cm}^3 \text{ g}^{-1})$$

Solid	P <sub>CO<sub>2</sub></sub> (bar)	Form	n (mmol g <sup>-1</sup> )	V <sub>pore</sub> (cm <sup>3</sup> g <sup>-1</sup> )
MIL-53(Fe)	3.5	INT	1.48	0.11
	40	NP	4.17	0.31
MIL-53(Fe)-Cl	60	NP	3.15	0.23
MIL-53(Fe)-Br	60	NP	2.84	0.21
MIL-53(Fe)-CH <sub>3</sub>	50	NP	2.80	0.21

### Computational assisted structure determination

The initial atomic positions for the different forms of the bare MIL-53(Fe) (CP, INT) were taken from the literature (Millange et al., 2008). Since the positions of the H atoms are not detected by X-ray diffraction, these atoms were added to the organic parts (C-H bond length of 1.14 Å and C-C-H angle of 120°) and to the μ<sub>2</sub>-O (O-H bond perpendicular to the Fe-O-Fe linkage with a bond length of 0.95 Å) using the Accelrys Material Studio Visualizer software (Accelrys, 2003). A geometry optimization based on the classical generic universal force field

(UFF) (Rappé et al., 1992) was then performed on the different structures. Such an approach has been successfully employed in the past to construct plausible structure models of a variety of MILs (Devic et al., 2010; Horcajada et al., 2011). Regarding the NP and LP forms of the MIL-53(Fe)-X ( $X=Cl, Br, CH_3$ ), we followed the same computational assisted structure determination strategy as described in our previous articles (Devic et al., 2010; Horcajada et al., 2011) using the unit cell parameters given in the Table 1 of the manuscript. The so-built structure models were further DFT geometry optimized in absence and in presence of  $CO_2$  as presented in the manuscript.

From the DFT optimized structures of MIL-53(Fe)-X ( $X=-, Cl, Br, CH_3$ ), it was also possible to extract the Mulliken charges for all the atoms of the framework as summarized in Table S1, the labels of the atoms being reported in Figure S5.

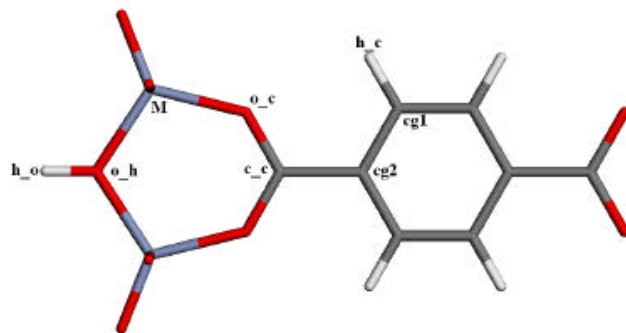


**Figure S6** Labels of the atoms for the MIL-53(Fe) ( $M$  is the metal center). In the modified MIL-53(Fe)-X structures,  $X$  replaces one  $h_c$ .

**Table S2.** Partial charges for all the atoms of the MIL-53(Fe)-X ( $X=-, Cl, Br, CH_3$ ).

Atoms	MIL-53(Fe)-H	MIL-53(Fe)-Br	MIL-53(Fe)-Cl	MIL-53(Fe)-CH <sub>3</sub>
<b>Fe</b>	1.210	1.142	1.146	1.152
<b>o_c</b>	-0.530	-0.520	-0.520	-0.530

<b>h_c</b>	0.145	0.170	0.160	0.120
<b>h_o</b>	0.308	0.350	0.380	0.320
<b>o_h</b>	-0.676	-0.685	-0.686	-0.680
<b>c_c</b>	0.572	0.575	0.580	0.550
<b>cg2</b>	-0.077	-0.018	-0.030	-0.020
<b>cg1</b>	-0.073	-0.060	-0.070	-0.073
<b>X</b>		-0.111	-0.060	-0.100
<b>C(CH<sub>3</sub>)</b>				0.100

### Intra-framework interactions in the CP forms

It has been previously shown that infrared spectroscopy was able to precisely characterize the bridged  $\mu_2$ -OH group of the functionalized MIL-53(Fe)s (Devic et al, 2010). In its activated form, MIL-53(Fe)-CH<sub>3</sub> presents a unique  $\nu(\text{OH})$  band at 3649 cm<sup>-1</sup> and a  $\delta(\text{OH})$  one at 843 cm<sup>-1</sup> (Figure 5), indicating the presence of hydroxyl groups in a single environment, free of any interaction. Alternatively, two  $\nu(\text{OH})$  bands appeared at 3648 and 3620 cm<sup>-1</sup> (broad) and two  $\delta(\text{OH})$  bands at 848 and 867 cm<sup>-1</sup> on MIL-53(Fe)-Cl and at 3650, 3592 (very broad) and 854, 874 cm<sup>-1</sup> on MIL-53(Fe)-Br. The bands at about 3650 cm<sup>-1</sup> and 850 cm<sup>-1</sup>, are assigned to the presence of hydroxyl groups free of any interaction, later denoted OH<sub>free</sub>. The other bands on these solids are assigned to hydroxyl groups hydrogen bonded to the halogen group (denoted OH<sub>X</sub>). This interaction appears stronger for MIL-53(Fe)-Br than for MIL-53(Fe)-Cl, as revealed by a lower  $\nu(\text{OH})$  and higher  $\delta(\text{OH})$  wavenumbers of the OH<sub>X</sub> (3592 instead of 3620 cm<sup>-1</sup> and 874 instead of 867 cm<sup>-1</sup> respectively). Such an observation is fully consistent

with the conclusions drawn from DFT simulations. Indeed in absence of CO<sub>2</sub>, the simulated CP forms of MIL-53(Fe)-X (X = Cl, Br) show the existence of hydrogen bonds between X and the  $\mu_2$ -OH group with characteristic distances (2.4-2.5 Å) (see Figures S6-S9). These interactions imply a rotation of the organic linker (labeled o\_c-c\_c-cg2-cg1) (12° for -Br, 8° for -Cl) compared to the structure of the parent MIL-53(Fe) (15°). Considering the Mulliken charges extracted for all the atoms of the MIL-53(Fe)-X frameworks (Table S2), one can deduce that the electrostatic interactions between X and the  $\mu_2$ -OH group are stronger in the case of MIL-53(Fe)-Br compared to its -Cl analogue. It is further observed that the simulated CP form (Figure S9) for MIL-53(Fe)-CH<sub>3</sub> does not show any significant interaction between the -CH<sub>3</sub> function and the  $\mu_2$ -OH group, in agreement again with the IR observations

**Grand Canonical Monte Carlo calculations to estimate the CO<sub>2</sub> adsorption enthalpies at low coverage in each NP form of the MIL-53-X (X = -, Br, Cl, CH<sub>3</sub>).**

Grand Canonical Monte Carlo (GCMC) simulations were performed using the Sorption module of Materials Studio (Accelrys, 2003) with typically  $2.0 \times 10^6$  Monte Carlo steps following  $2 \times 10^6$  steps for equilibration. The Ewald summation was used for calculating the electrostatic interactions while the short-range contributions were computed with a cutoff distance of 12 Å. The simulations were conducted at 300 K using the DFT optimized NP structures of each investigated MIL-53(Fe), considering simulation boxes as 32 unit cells.

The Lennard Jones potential parameters for the framework atoms of MOFs were taken from the Universal (UFF) force field Rappé et al., 1992) while the CO<sub>2</sub> molecule was treated by a rigid linear triatomic model with three charged LJ interaction sites developed by Harris and Yung model (Harris and Yung (1995). The adsorbate/adsorbent LJ interatomic potential

parameters were then calculated using Lorentz Berthelot mixing rules. The interactions between CO<sub>2</sub> and the surface of the MIL-53(Fe) series were described by a combination of site-site LJ and Coulombic potentials. The Mulliken charges carried by all the atoms of the MIL-53(Fe) framework are those reported in Table S1. The differential adsorption enthalpy for CO<sub>2</sub> at low coverage was calculated in all these forms, through the fluctuation over the number of particles in the system and from the internal energy (Frenkel and Smit, 1996). The corresponding values are reported in Table S2.

**Table S3.** Adsorption enthalpies (in kJ.mol<sup>-1</sup>) for CO<sub>2</sub> in the NP forms of all the investigated MIL-53(Fe)-X (X=-, Br, Cl, CH<sub>3</sub>) at low coverage.

X	ΔH <sub>ads</sub> (kJ mol <sup>-1</sup> )
H	-45
Br	-46
Cl	-43
CH <sub>3</sub>	-43,5

**Estimation of the pore volume of the MIL-53(Fe)-X (X = -, Cl, Br, CH<sub>3</sub>) from simulations.**

The free volume was calculated for all structures using a method of trial insertions within the entire volume of the unit cell. A probe size of 0 Å was used to determine the total free volume corresponding to the volume of the simulated cell that is not occupied by framework atoms.

The methodology has been described by Frost et al. (2006). The results are given in the article (Table 2).

**Arrangement of the CO<sub>2</sub> molecules in the NP forms of MIL-53(Fe)-X (X=-, Br, Cl, CH<sub>3</sub>) Series.**

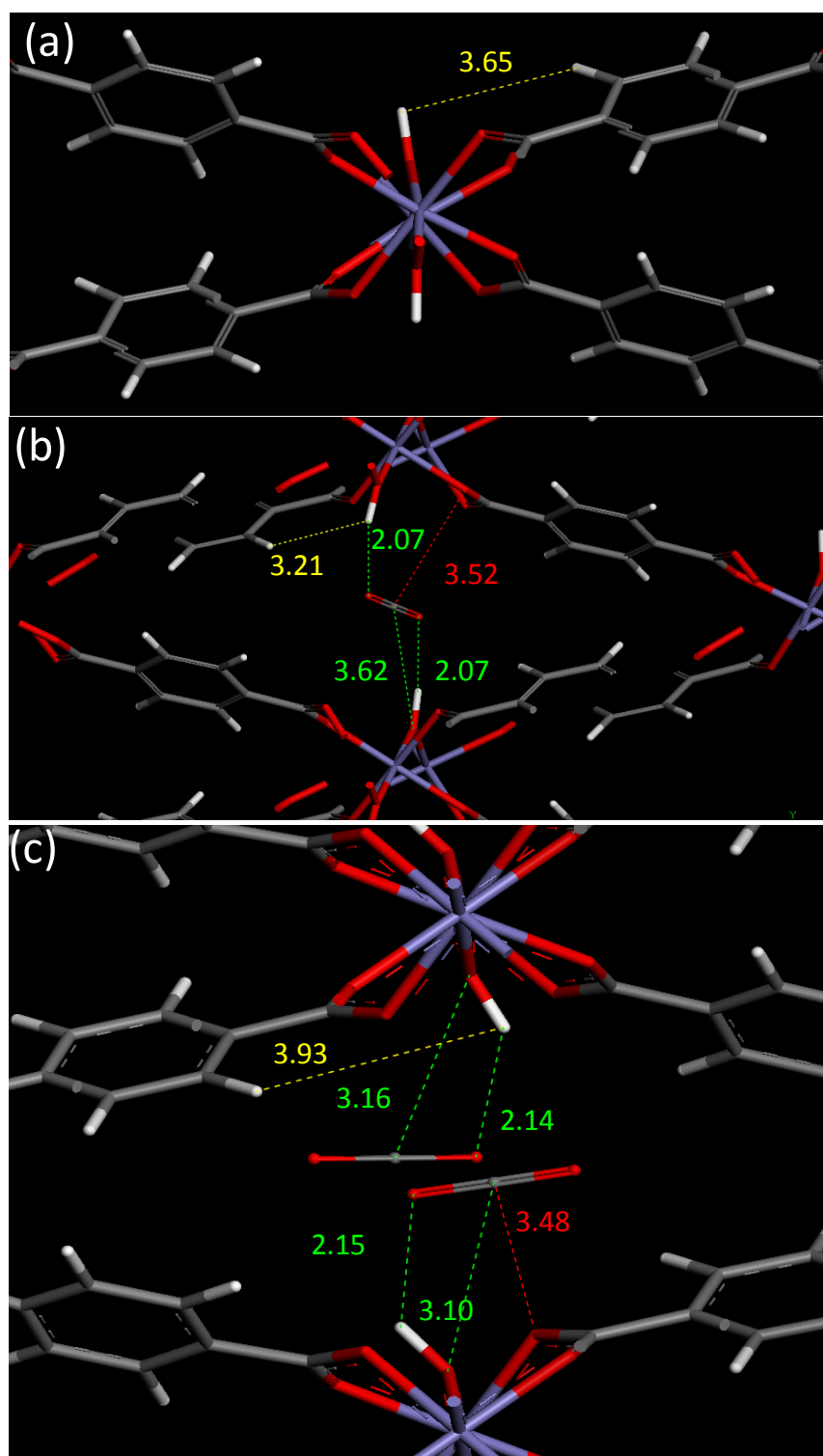


**Figure S7.** DFT optimized arrangements of  $\text{CO}_2$  in the NP form of MIL-53(Fe): case of 1 (b) and 2 (c) molecules per pore. Comparison with the DFT optimized structures in absence of  $\text{CO}_2$  (a). The distances for  $\mu_2\text{-OH}\cdots\text{CO}_2$  (in green),  $\mu_2\text{-OH}\cdots\text{X}$  (in yellow) and  $\text{CO}_2\cdots\text{O}$  (carboxylate) are reported.

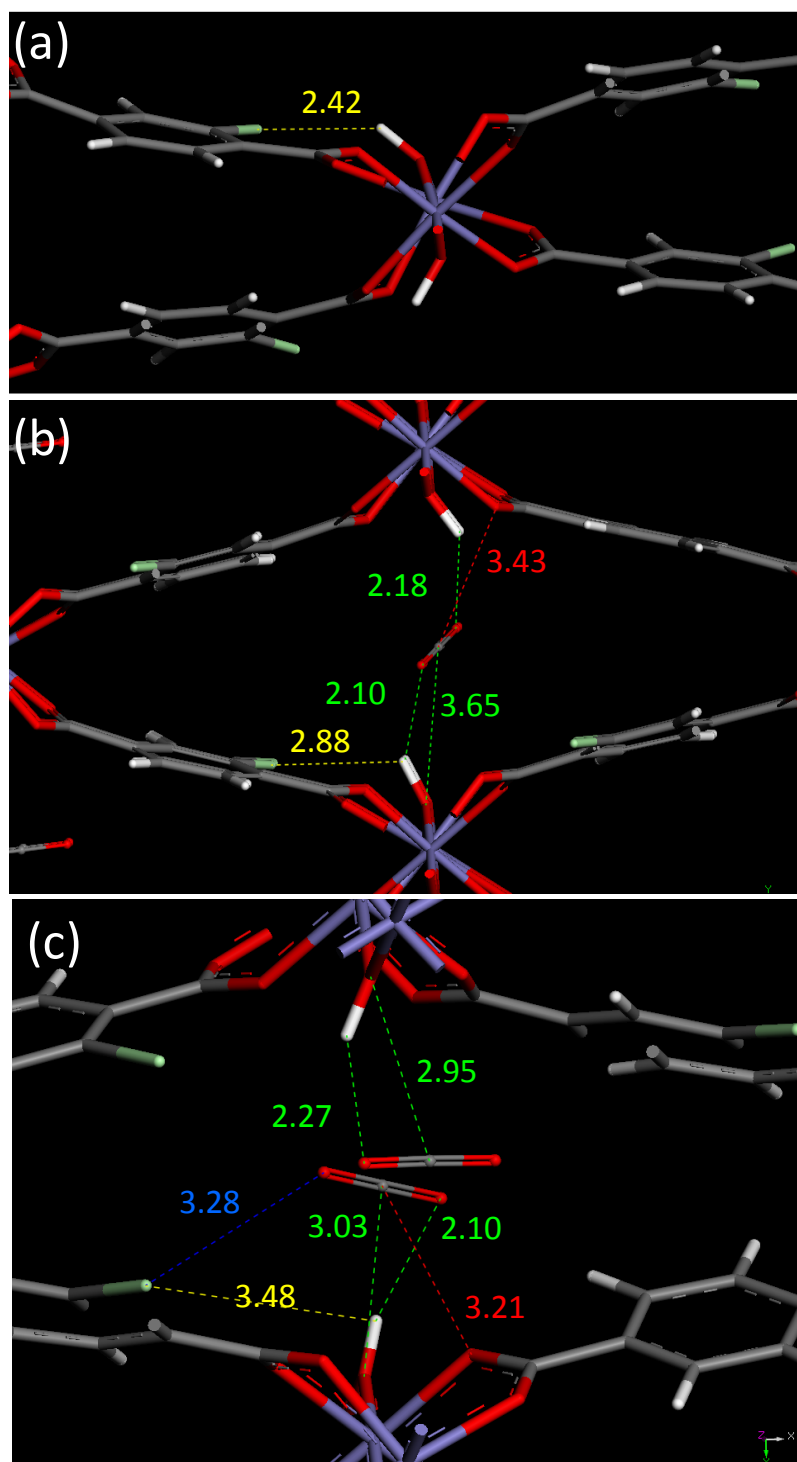


**Figure S8.** DFT optimized arrangements of  $\text{CO}_2$  in the NP form of MIL-53(Fe)-Cl: case of 1 (b) and 2 (c) molecules per pore. Comparison with the DFT optimized structures in absence of

CO<sub>2</sub> (a). The distances for  $\mu_2\text{-OH}\cdots\text{CO}_2$  (in green),  $\mu_2\text{-OH}\cdots\text{X}$  (in yellow), CO<sub>2</sub> $\cdots\text{X}$  (in blue) and CO<sub>2</sub> $\cdots\text{O}$  (carboxylate) (in red) are reported.

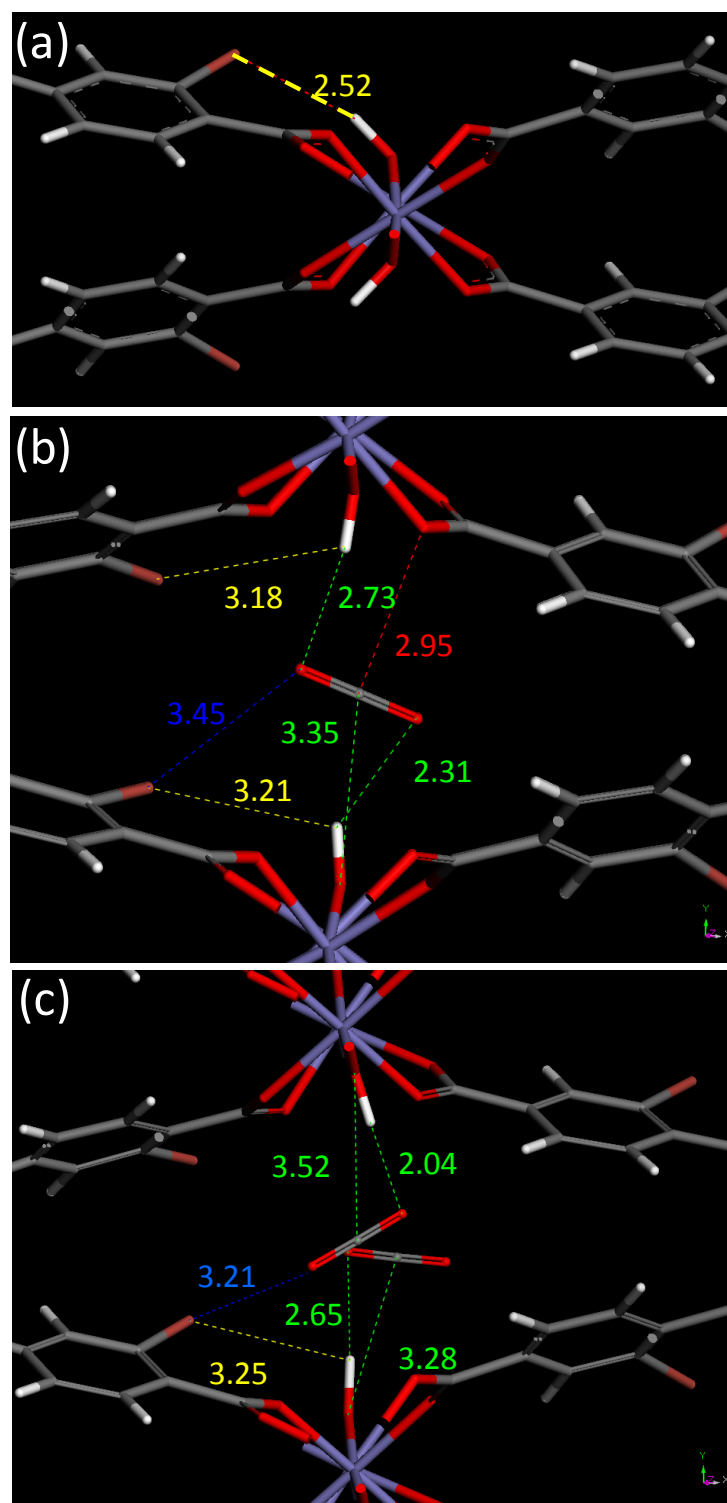


**Figure S9.** DFT optimized arrangements of CO<sub>2</sub> in the NP form of MIL-53(Fe)-Br: case of 1 (b) and 2 (c) molecules per pore. Comparison with the DFT optimized structures in absence of

CO<sub>2</sub> (a). The distances for  $\mu_2\text{-OH}\cdots\text{CO}_2$  (in green),  $\mu_2\text{-OH}\cdots\text{X}$  (in yellow), CO<sub>2</sub> $\cdots\text{X}$  (in blue) and CO<sub>2</sub> $\cdots\text{O}$  (carboxylate) (in red) are reported.

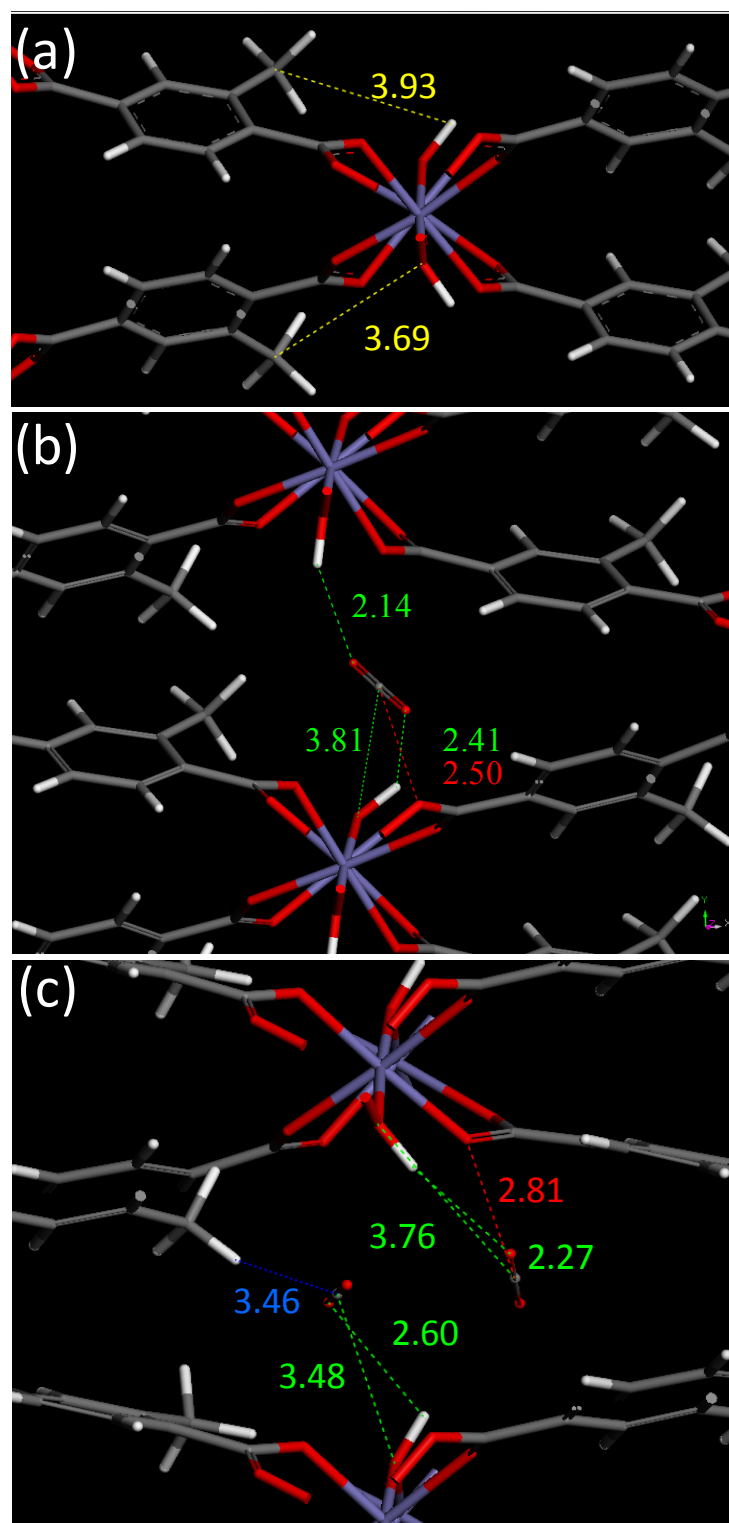


**Figure S10.** DFT optimized arrangements of CO<sub>2</sub> in the NP form of MIL-53(Fe)-CH<sub>3</sub>: case of 1 (b) and 2 (c) molecules per pore. Comparison with the DFT optimized structures in absence of CO<sub>2</sub> (a). The distances for  $\mu_2\text{-OH}\cdots\text{CO}_2$  (in green),  $\mu_2\text{-OH}\cdots\text{X}$  (in yellow), CO<sub>2</sub> $\cdots\text{X}$  (in blue) and CO<sub>2</sub> $\cdots\text{O}$  (carboxylate) (in red) are reported.

## **References.**

Accelrys Inc., San Diego, CA, 2003

T. Devic, P. Horcajada, C. Serre, F. Salles, G. Maurin, B. a. Moulin, D. Heurtaux, G. Clet, A. Vimont, J.-M. Grenache, B. L. Ouay, F. Moreau, E. Magnier, Y. Filinchuk, J. m. Marrot, J.-C. Lavalley, M. Daturi and G. Férey, *J. Am. Chem. Soc.*, 2010, **132**, 1127-1136.

Frenkel, D., Smit, B. Understanding Molecular Simulation; Academic Press: San Diego, CA, 1996.

H. Frost, T. Düren, R.Q. Snurr, *J. Phys. Chem. B*, 2006, **110**, 9565-9570

J.G. Harris, K.H. Yung, *J. Phys. Chem.*, 1995, **99**, 12021, 12024

P. Horcajada, F. Salles, S. Wuttke, T. Devic, D. Heurtaux, G. Maurin, A. Vimont, M. Daturi, O. David, E. Magnier, N. Stock, Y. Filinchuk, D. Popov, C. Riekel, G. Férey, C. Serre, *J. Am. Chem. Soc.*, 2011, **133**, 17839-17847.

F. Millange, N. Guillou, R.I. Walton, J.M. Grenèche, I. Margiolaki, G. Ferey, *Chem. Commun.* 2008, 4732-4734.

K. Rappé, C.J. Casewit, K.S. Colwell, W.A. Goddard III, W.M. Skiff, *J. Am. Chem. Soc.* 1992, **114**, 10024-10035.